

# DIRICHLET SPHERES IN CONTINUUM QUANTUM FIELD THEORY\*

H. WEIGEL

*Fachbereich Physik, Universität Siegen,*

*Walter-Flex-Straße 3, D-57068 Siegen*

*E-mail: weigel@physik.uni-siegen.de*

We study the vacuum polarization (Casimir) energy in renormalizable, continuum quantum field theory in the presence of a background field, designed to impose Dirichlet boundary conditions on the fluctuating quantum field. In two and three spatial dimensions the Casimir energy diverges as a background field becomes concentrated on the surface on which the Dirichlet boundary condition would eventually hold. This divergence does not affect the force between rigid bodies, but it does invalidate calculations of Casimir stresses based on idealized boundary conditions.

## 1 Introduction and Motivation

This presentation is based on work done in collaboration<sup>1</sup> with N. Graham, R. L. Jaffe, V. Khemani, M. Quandt, and O. Schröder.

The interaction of fluctuating quantum fields with background fields gives rise to vacuum polarization energies because the zero-point energies change. Colloquially these vacuum polarization energies are called Casimir energies. In this talk I present calculations<sup>1</sup> of Casimir energies for extreme cases when a static background field in  $D$  spatial dimensions,  $\sigma(\vec{x})$ , imposes Dirichlet boundary conditions on the fluctuating quantum field,  $\phi(t, \vec{x})$ , in some subspace  $\mathbb{S} \subset \mathbb{R}^D$ :  $\phi(t, \vec{a}) = 0$  for  $\vec{a} \in \mathbb{S}$ . These calculations are afflicted with severe divergences which fall into two categories: (i) ultraviolet divergences in quantum field theory and (ii) those due to singularities of the background fields. Although the vacuum polarization energy cannot be reliably computed from only the low order Feynman diagrams, the type (i) divergences can be identified thereof. The type (ii) divergences are due to large Fourier components carried by the background fields. In reality the contributions of these components to the vacuum polarization energy are suppressed by the dynamics of the interaction of some material with the quantum field. We therefore label these divergences *quantum* and *material* divergences for type (i) and (ii), respectively. It is essential to disentangle the quantum and material divergences since no reliable conclusion can be drawn from a calculation that does not have the material divergences under control.

As is reviewed in Ref.<sup>2</sup> the existence of scattering data for the interaction of the quantum field with the background allows us to unambiguously compute the corresponding vacuum polarization energy<sup>a</sup>. In particular, the

---

\*Talk presented at the QFEXT03 Workshop, Norman, Oklahoma, September 2003.

<sup>a</sup>See also the contributions by R.L. Jaffe and M. Quandt to these proceedings. A detailed derivation is given in Ref.<sup>3</sup>.

associated quantum divergences are under control when the theory that describes this interaction is renormalizable. Hence we can compute the Casimir energy for any (piecewise) continuous background field. The strategy to explore the material divergences is thus to consider a background field that in a particular, singular limit imitates a Dirichlet boundary condition. Most importantly, the vacuum polarization energy is computed *before* that singular limit is assumed. We then study the vacuum polarization energy as a function of the parameters that regulate this singular limit. To be specific, the Dirichlet boundary condition at a point  $\vec{a}$  is imitated by a delta-function background,  $\sigma(\vec{x}) = \lambda\delta(\vec{x} - \vec{a})$  in the *strong* limit,  $\lambda \rightarrow \infty$ . We parameterize the delta-function with the help of a finite width,  $\Delta$ , via

$$\begin{aligned}\sigma_{\perp}(z) &= \frac{\lambda}{\Delta} \left( \theta(z + \Delta/2) - \theta(z - \Delta/2) \right) \\ \sigma_{\parallel}(z) &= \frac{\lambda}{\Delta} \left( \theta(|z| - L + \Delta/2) - \theta(|z| - L - \Delta/2) \right) \\ \sigma_{\circ}(r) &= \frac{3\lambda/4\pi}{(R + \Delta)^3 - R^3} \left( \theta(r - R) - \theta(r - R - \Delta) \right)\end{aligned}\tag{1}$$

for the cases of a single plate, two plates at distance  $2L$ , and a sphere of radius  $R$  in three spatial dimensions, respectively. For plates the total number of spatial dimensions is of lesser importance as we only consider the energy per unit area. The above slab-type parameterizations of the delta-functions in various geometries are advantageous because they have simple Fourier transforms,


$$\tilde{\sigma}(\vec{p}) = \int d^D x e^{i\vec{p}\cdot\vec{x}} \sigma(\vec{x})\tag{2}$$

for all spatial dimensions  $D$ . For any  $\lambda < \infty$  and  $\Delta > 0$  the vacuum polarization energy can unambiguously be computed with the techniques of Refs. <sup>2,3</sup>. The *sharp* limit ( $\Delta \rightarrow 0$ ) imitates the delta-function background. The subsequent *strong* limit imposes the Dirichlet condition. This calculation is different from a pure boundary condition calculation which assumes both the sharp and the strong limits *before* computing the vacuum polarization energy<sup>4</sup>.

As motivated above, we study the low order Feynman diagrams to analyze the emergence of material divergences in the sharp limit. For this we consider a bosonic quantum field whose interaction with the static background field is given by the Lagrangian  $\mathcal{L}_{\text{int}} = \frac{-1}{2}\sigma(\vec{x})\phi^2$ .

## 2 The Tadpole Graph

Let us start the discussion of low order contribution to the vacuum polarization energy by considering the tadpole diagram



$$\text{---}\sigma(\vec{x})\text{---} \bigcirc = E^{(1)} = \int d^D x \sigma(\vec{x}) \int \frac{d^n l}{(2\pi)^n} \frac{i}{l^2 - m^2}\tag{3}$$

which we have written in dimensional regularization, *e.g.*  $n$  may be fractional while  $D$  is an integer. It is actually important, not to include the background into dimensional regularization because renormalization occurs on the level of Green's functions which do not involve the background fields. We recognize that spatial and loop integration factorize, *i.e.* the tadpole diagram is local. Within the non-tadpole renormalization condition the counterterm contribution therefore exactly cancels  $E^{(1)}$  regardless of the details of  $\sigma(\vec{x})$ . Thus it is obvious that there are no further divergences at this order.

### 3 The Two-Point-Function

We will now study the two-point-function for which analytical results are also available. There is no quantum divergence at this order in two spatial dimensions and the diagram can straightforwardly be computed

$$\sigma(\vec{x}) \cdots \text{(circle)} \cdots \sigma(\vec{x}) = E_{2\text{D}}^{(2)}[\sigma] = -\frac{\lambda^2}{16\pi} \int \frac{d^2 p}{(2\pi)^2} \tilde{\sigma}(\vec{p}) \tilde{\sigma}(-\vec{p}) \frac{1}{|\vec{p}|} \arctan \frac{|\vec{p}|}{2m}. \quad (4)$$

It is then straightforward to extract the most singular contribution to the vacuum polarization energy per unit length

$$\mathcal{E}_{2\text{D}}^{(2)}(\sigma) = \frac{1}{32\pi} \ln(\Delta m) + \text{terms finite for } \Delta \rightarrow 0 \quad (5)$$

for a single plate, *cf.* eq. (1). Obviously this contribution diverges logarithmically in the sharp limit. A quadratic counterterm, that would anyhow not be required by any quantum divergence, diverges like  $1/\Delta$  and thus does not remove this divergence.

In three spatial dimensions the two-point-function has a quantum divergence which is manifest in the polarization tensor

$$p \cdots \text{(circle)} \cdots p = \Pi(p^2) = \int \frac{d^n l}{(2\pi)^n} \frac{1}{l^2 - m^2} \frac{1}{(l - p)^2 - m^2}. \quad (6)$$

The associated divergences are removed by a quadratic counterterm  $\mathcal{L}_{\text{CT}} \propto \Pi(-\mu^2)\sigma^2$ , whose coefficient is entirely given by the polarization tensor and thus is the *same* for all background fields. This independence is an essential feature of renormalization: counterterm coefficients are fixed by a (chosen) condition but not modified when the background changes. Then the second order contribution to the renormalized vacuum polarization energy is then easily computed by contracting the renormalized vacuum polarization tensor with the Fourier transform of the background field. To be concise, we only display the result for the case that the fluctuating field is massless

$$E_{3\text{D}}^{(2)}[\sigma] = \frac{1}{64\pi^2} \int \frac{d^3 p}{(2\pi)^3} \tilde{\sigma}(\vec{p}) \tilde{\sigma}(-\vec{p}) \ln \frac{\vec{p}^2}{\mu^2}. \quad (7)$$

For the geometry of two parallel plates with separation  $2L$  this yields

$$\mathcal{E}_{3D}^{(2)}[\sigma_{\parallel}] = -\frac{\lambda^2}{16\pi^2\Delta} \left\{ \ln(\Delta\mu) + \gamma - 1 + \frac{\Delta}{4L} + \mathcal{O}\left(\frac{\Delta^2}{L^2}\right) \right\} \quad (8)$$

for the energy  $\mathcal{E} = E/A$  per unit area  $A$ . We observe a  $\ln \Delta / \Delta$  singularity in the sharp limit. This singularity, however, is just twice the one for a single plate and it does not depend on the separation of the two plates. Hence the force (density)  $\partial\mathcal{E}/\partial L$  does not diverge in the sharp limit.

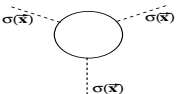
The situation is different for the sphere,

$$E_{3D}^{(2)}[\sigma_{\circ}] = \frac{-\lambda^2}{128\pi^3 R^2} \left( \frac{1}{\Delta} (\ln(\mu\Delta) + \gamma - 1) - \frac{\ln(\mu\Delta)}{R} \right) + \dots, \quad (9)$$

where the ellipses represent contributions that are finite as  $\Delta \rightarrow 0$ . Again we observe a  $\ln \Delta / \Delta$  singularity in the sharp limit. This time, however, the singularity depends on the radius of the sphere. Thus the stress  $\partial\mathcal{E}/\partial R$  does in fact diverge and remains ill-defined within a pure boundary condition calculation; the width  $\Delta$  cannot approach zero. Rather it is bounded by some material properties.

#### 4 The Three-Point-Function

In case of the three-point-function

$$E^{(2)}[\sigma] = \text{Diagram} \quad (10)$$


only numerical results are available. For the parallel plates geometry they are listed in table 1. Essentially we observe a logarithmic divergence in the sharp limit. Here the divergence is less severe than for the two point function which indicates that the higher order contributions are actually finite. This will be discussed in section 5. The important result is that this divergence is independent of the separation of the two plates implying that the force has a finite sharp limit. Also for the spherical shell we find a logarithmic singularity as the sharp limit is approached. This is shown in figure 1. In this case, however, the divergent term depends on the radius of the shell and thus the resulting stress,  $\partial E/\partial R$  is also divergent, as already observed for the two-point-function contribution to the vacuum polarization energy. One might want to argue that a suitable constant of proportionality in the definition of the spherical background field,  $\sigma_{\circ}$ , in eq. (1) might yield a finite force. However, this cannot be achieved for both the two- and three-point-function contributions<sup>1</sup>.

The results obtained so far generalize: The renormalized vacuum energies always diverge in the boundary condition limit while forces between rigid bodies have a finite sharp limit because the singularities are (material) properties

Table 1. The three point function contribution to the energy density for two parallel plates  $\mathcal{E}^{(3)}[\sigma_{\parallel}]$  as a function of their separation ( $2L$ ) and the width of the slabs ( $\Delta$ ), *cf.* eq. (1). Factors that are independent of  $L$  or  $\Delta$  have been omitted. Dimensions are set by the mass of the fluctuating quantum field.

$\Delta$	$L = 0.5$	$L = 0.8$	$L = 1.0$	$L = 1.2$	$L = 1.5$
0.010	-163.04	-160.24	-160.88	-161.04	-161.28
0.025	-122.16	-119.68	-119.68	-119.76	-120.00
0.050	-95.36	-92.64	-92.16	-92.08	-92.24
0.100	-70.56	-67.84	-67.36	-67.28	-67.20
0.200	-48.08	-44.72	-45.12	-45.04	-44.96

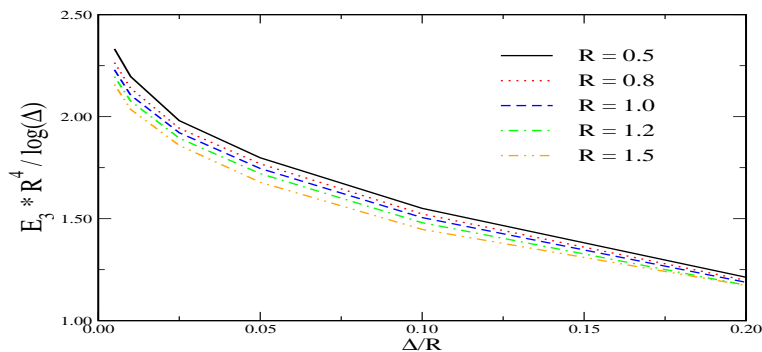


Figure 1. The three–point–function contribution to the vacuum polarization energy of a spherical shell,  $E_3^{(3)}[\sigma_{\circ}]$  as a function of the inner radius ( $R$ ) and the width ( $\Delta$ ) of the shell, *cf.* eq. (1). Factors that are independent of  $L$  or  $\Delta$  have been omitted. Dimensions are set by the mass of the fluctuating quantum field.

of the individual objects. However, for stresses that arise from deformations of such objects the singularities do not drop out.

## 5 The Sharp Limit at $n^{\text{th}}$ order

In this section we will take a different venue and adopt the sharp limit first and compute Feynman diagrams for the vacuum polarization energy. These diagrams are potentially divergent and we regularize with a sharp cutoff  $\Lambda$ . As indicated in the previous section this shows that diagrams of large enough order indeed do not diverge in the sharp limit. Note, however, that this procedure does not make contact with renormalization theory, in fact, we do not renormalize at all. Rather it is an efficient way to localize the divergences for delta–function type background potentials. For such special potentials it is convenient to use Green’s functions in coordinate space when evaluating

Feynman diagrams. Details of these calculations are given in Ref.<sup>1</sup>. Here we content ourselves with listing the results.

First, we consider two parallel plates in three spatial dimensions. The corresponding background in the sharp limit is  $\sigma_{\parallel}^*(\vec{x}) = \lambda [\delta(z - L) + \delta(z + L)]$ . Then the  $n^{\text{th}}$  order contribution to the energy density per unit area is ( $\omega(q) = \sqrt{q^2 + m^2}$ )

$$\mathcal{E}_{\Lambda}^{(n)}[\sigma_{\parallel}^*] = \frac{-1}{2n} \int^{\Lambda} \frac{d^3q}{(2\pi)^3} \left[ \frac{-\lambda}{2\omega(q)} \right]^n \left\{ (1 + e^{-2\omega(q)L})^n + (1 - e^{-2\omega(q)L})^n \right\}. \quad (11)$$

Simple power counting shows that there are divergences at orders  $n = 1, 2$  and  $3$ , which are regulated by the sharp cutoff  $\Lambda$ . The dependence on the separation is exponentially suppressed and thus the divergences are separation independent. The orders  $n \geq 4$  are finite. Obviously this matches our expectations from the previous sections. Actually the Feynman series (11) can be summed:

$$\mathcal{E}_{\Lambda}[\sigma_{\parallel}^*] = \int_m^{\sqrt{\Lambda^2 + m^2}} \frac{dt}{(2\pi)^2} t \sqrt{t^2 - m^2} \ln \left[ 1 + \frac{\lambda}{t} + \frac{\lambda^2}{4t^2} (1 - e^{-4tL}) \right]. \quad (12)$$

The same result is found within the interface formalism<sup>5</sup>. We can now compute a regularize pressure,

$$\mathcal{P}_{\Lambda}[\sigma_{\parallel}^*] = -\frac{1}{2} \frac{\partial \mathcal{E}_{\Lambda}[\sigma_{\parallel}^*]}{\partial L} = -\frac{\lambda^2}{8\pi^2} \int_m^{\sqrt{\Lambda^2 + m^2}} dt \frac{\sqrt{t^2 - m^2} e^{-4tL}}{1 + \frac{\lambda}{t} + \frac{\lambda^2}{4t^2} (1 - e^{-4tL})}, \quad (13)$$

which does not diverge as  $\Lambda \rightarrow \infty$ . Moreover, we can take the strong limit  $\lambda \rightarrow \infty$  and find the boundary condition calculation result<sup>6</sup> for the force between Dirichlet plates. This is expected, as the boundary condition approach is reliable for the force between rigid bodies.

We now repeat this exercise for the spherical shell, *i.e.*  $\sigma_{\circ}^*(\vec{x}) = \lambda \delta(r - R)/4\pi R^2$  and find

$$E_{\Lambda}^{(n)}(\sigma_{\circ}^*) = \frac{2}{n} \left( \frac{-\lambda}{4\pi R} \right)^n \int_0^{\Lambda} \frac{d\omega}{2\pi} I_n \left( R\sqrt{\omega^2 + m^2} \right) \\ I_n(z) = \sum_{\ell} (2\ell + 1) [I_{\ell+1/2}(z) K_{\ell+1/2}(z)]^n. \quad (14)$$

The divergence structure of the momentum integral is dictated by the large  $z$  behavior of the sum  $I_n(z)$  which is shown for  $n = 2, 3$  and  $4$  in figure 1. The sum  $I_1(z)$  is actually divergent before integrating over the momentum. However, this is not a severe problem because this contribution to the vacuum polarization energy is completely canceled in the no-tadpole renormalization scheme. We see from figure 1 that  $I_n(z) \propto z^{-\alpha_n}$ . Numerically we find  $\alpha_2 = 0.21$ ,  $\alpha_3 = 1.00$  and  $\alpha_4 = 1.99$ . That is, the second order contribution has a more severe singularity at large cutoff than just logarithmically which was expected from the quantum divergence. This reflects the singular sharp limit

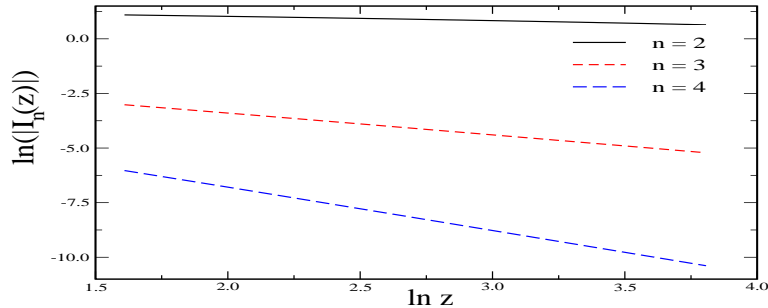


Figure 2. Double logarithmic plot of the orbital angular momentum sum in eq. (14).

that dwells on top of the quantum divergence. The third order contribution is logarithmically divergent in support of the numerical result presented in the previous section. Contributions of order four and higher are finite as  $\Lambda \rightarrow \infty$ . The important information is that the stress  $\partial E_\Lambda / \partial R$  is also ultraviolet divergent. That is, the cutoff must be kept finite which is achieved by taking material properties into account.

The expansion (14) can formally be summed leading to the same expression as found in the boundary condition approach<sup>7</sup>. However, that is still a divergent quantity when the cutoff is removed.

## 6 Conclusions

We have computed the Casimir energy of a Dirichlet boundary from singular limits of Casimir energies of (piecewise) continuous background fields. For the latter, the Casimir energy can be calculated using standard renormalization tools of quantum field theory. Although these energies are finite and unambiguous for any particular smooth background, the limit  $\Delta \rightarrow 0$ , when the background becomes sharp and concentrated on the boundary, can still diverge. For three space dimensions, the Casimir energy has  $\frac{1}{\Delta} \ln \Delta$  divergences both for parallel plates and for the sphere. These divergences arise from large Fourier modes of the background field and should not be confused with the loop divergences of Feynman diagrams: the former also appear in diagrams that have no quantum divergences. In particular, the third order diagram needs no renormalization but also diverges in the sharp limit, going like  $\ln \Delta$ .

This cutoff dependence may or may not enter into physically measurable quantities. The force between rigid bodies is never affected, so our analysis does not alter standard results such as the force between parallel plates. However, it does render meaningless calculations of stresses, such as the Casimir surface tension of the sphere. Such quantities are cutoff dependent, and cannot be defined independently of the material properties that determine the

cutoff.

We expect that these results generalize to the electromagnetic case. Thus they invalidate Boyer's result<sup>8</sup> that the conducting sphere experiences a cutoff-independent, repulsive Casimir stress. For such a statement to hold, it is necessary to show that it can be obtained as the limit of an underlying smooth, renormalizable quantum field theory. Otherwise, the Boyer problem cannot be studied without reference to material properties, and the assertion that sphere has repulsive Casimir force is unwarranted.

### Acknowledgments

I would like to thank the organizers, especially Kim Milton, for providing this interesting workshop. This work has been supported in parts by the Deutsche Forschungsgemeinschaft (DFG) under contract We 1254/6-1.

### References

1. N. Graham, *et al.*, arXiv:hep-th/0309130.
2. N. Graham, R.L. Jaffe and H. Weigel, *Int. J. Mod. Phys. A* **17**, 846 (2002)
3. N. Graham *et al.*, *Nucl. Phys. B* **645**, 49 (2002); *Phys. Lett. B* **572**, 196 (2003).
4. For reviews and many references see: V.M. Mostepanenko and N.N. Trunov, *The Casimir Effect and its Application*, Clarendon Press, Oxford (1997); K.A. Milton, *The Casimir Effect: Physical Manifestations Of Zero-Point Energy*, River Edge, USA: World Scientific (2001);
5. N. Graham, R. L. Jaffe, M. Quandt and H. Weigel, *Phys. Rev. Lett.* **87**, 131601 (2001).
6. M. Bordag, D. Hennig and D. Robaschik, *J. Phys. A* **25**, 4483 (1992).
7. K.A. Milton, *Phys. Rev. D* **68**, 065020 (2003)
8. T.H. Boyer, *Phys. Rev.* **174**, 1764 (1968).